

Swift Observations of the highly X-ray variable Narrow Line Seyfert 1 galaxy RX J0148.3–2758

Dirk Grupe¹

grupe@astro.psu.edu

, Karen M. Leighly², Stefanie Komossa³, Patricia Schady^{1,4}, Paul T. O'Brien⁵, David N. Burrows¹, John A. Nousek¹
dxb15@psu.edu, nousek@astro.psu.edu

ABSTRACT

We report on *Swift* observations of the Narrow-Line Seyfert 1 galaxy (NLS1) RX J0148.3–2758. It was observed for 41.6 ks in 2005 May and for 15.8 ks in 2005 December. On short as well as on long timescales RX J0148.3–2758 is a highly variable source. It doubles its X-ray flux within 18–25 ks. The observation of 2005 December 09, which had a flux 4 times lower than during the 2005 May observations, shows a significant hardening of the X-ray hardness ratio compared with the 2005-May and 2005–December 20/21 observations. A detailed analysis of the X-ray spectra shows that we actually observe two spectral changes in RX J0148.3–2758: First a decrease of the soft X-ray component between 2005 May and December 09, which is most likely due to an increase of the intrinsic absorber column, and second a decrease of the hard X-ray flux in the December 20/21 observations. The soft X-ray spectral slope $\alpha_{X,soft}=2.58^{+0.15}_{-0.12}$ during the high state in 2005 May agrees well with that measured by ROSAT ($\alpha_{X,soft}=2.54\pm0.82$). This soft X-ray spectrum is superimposed over a hard X-ray component with $\alpha_{X,hard}=0.96^{+0.15}_{-0.12}$ which is consistent with the hard X-ray spectral slope $\alpha_{X,hard}=1.11^{+0.16}_{-0.19}$ found by ASCA. The soft X-ray slope $\alpha_{X,soft}=1.93\pm0.58_{-0.42}$ measured during the December 09 observation, agrees well with $\alpha_{X,soft}=2.03^{+0.23}_{-0.20}$ measured from the ASCA observation when RX J0148.3–2758 was also in a low state. In contrast to the strong X-ray variability, the analysis of the *Swift* UVOT photometry from December 2005 of RX J0148.3–2758 shows no significant variability in any of the 6 UVOT filters. From the simultaneous X-ray and UV observations in 2005 December we measured the X-ray loudness α_{ox} varies between $\alpha_{ox}=1.5$ and 1.8. Our *Swift* observations of RX J0148.3–2758 demonstrate the great potential the multi-wavelength observatory *Swift* has for AGN science.

Subject headings: galaxies: active, galaxies: individual (RX J0148.3–2758)

1. Introduction

Most of the power in the spectral energy distribution (SED) of an AGN is deposit in the Big Blue Bump (BBB, Shields 1978). As suggested by Walter & Fink (1993), the BBB may stretch from the UV into the soft X-ray regime. The soft X-ray part of the BBB may be UV photons from the accretion disk which are shifted into the soft X-

¹Department of Astronomy and Astrophysics, Pennsylvania State University, 525 Davey Lab, University Park, PA 16802

²Department of Physics and Astronomy, University of Oklahoma, 440 West Brooks Street, Norman, OK 73019; email: leighly@nhn.ou.edu

³MPG für extraterrestrische Physik, Giessenbachstr., D-85748 Garching, Germany; email: skomossa@mpe.mpg.de

⁴Mullard Space Science Laboratory, Holmbury St. Mary, Dorking, Surrey RH5 6NT, U.K.; email: ps@mssl.ucl.ac.uk

⁵Department of Physics & Astronomy, University of Le-

icester, Leicester, LE1 7R, UK, email: pto@star.le.ac.uk

ray band by Comptonization in the accretion disk corona (e.g. Pounds et al. 1995). Based on their soft X-ray selected ROSAT AGN sample, Grupe et al. (1998a) showed that the BBB even extends into the optical and that sources with steeper X-ray spectra tend to have bluer optical spectra, suggesting that Narrow Line Seyfert 1 galaxies are the AGN with the strongest BBB component. However, from a study of the IUE spectra of NLS1s, Rodríguez-Pascual et al. (1997) came to the conclusion that NLS1s have weaker UV emission than Broad Line Seyfert 1s. All these studies, however, were hampered by the lack of simultaneity of the optical/UV and X-ray observation. Often these observations were performed years apart. This situation has changed now with the availability of the multi-wavelengths observatories XMM-Newton and *Swift*.

Equipped with three telescopes, the Burst Alert Telescope (BAT, Barthelmy 2005), the X-Ray Telescope (XRT, Burrows et al. 2005), and the UV-Optical Telescope (UVOT, Roming et al. 2005), *Swift* (Gehrels et al. 2004) is a multi-wavelength mission covering the electromagnetic spectrum between 6000Å at the low-energy end to 150 keV at the high-energy end. *Swift* was launched on 20-November-2004 in order to hunt for Gamma-Ray Bursts (GRBs). At the low-energy side of *Swift*'s observing window, the UVOT covers the wavelengths range between 1700-6000Å. The UVOT is a sister instrument of XMM's Optical Monitor (OM, Mason et al. 2001). The UVOT has a similar set of filters as the OM (Mason et al. 2001; Roming et al. 2005). The 0.3-10.0 keV range is covered by the XRT which uses a CCD detector identical to the EPIC MOS on-board XMM (Turner et al. 2001). As described by Hill et al. (2004) the XRT operates in three observing modes, the Photon Counting (PC) which is equivalent to the full-frame mode on XMM, Window Timing (WT), and Low-Rate Photo-diode mode (LrPD). Due to the nature of the *Swift* mission, the XRT switches automatically between the observing modes according to the brightness of a source. Only for specific purposes, e.g. in case of calibration observations, the modes are set manually in the observing schedule. At the high-energy part of *Swift*'s observing window, the BAT, which is a coated mask experiment, operates in the 15-150 keV energy range.

Even though the main purpose of the *Swift* mission is to detect and observe GRBs, part of the observing time on *Swift* is used for fill-in targets which fit into the schedule if no GRBs are observable. Because of its UV and X-ray capacities and its flexible scheduling *Swift* is the ideal observatory to study AGN.

With the launch of the X-ray satellite ROSAT (Trümper 1982) the X-ray energy range down to 0.1 keV became accessible for the first time. During the half year ROSAT All-Sky Survey (RASS, (RASS, Voges et al. 1999) a large number of sources with steep X-ray spectra were detected (Thomas et al. (1998); Beuermann et al. (1999); Schwope et al. (2000)). About one third to one half of these sources are AGN. Grupe (1996) and Grupe et al. (1998a, 2004a) found that about 50% of bright soft X-ray selected AGN are Narrow-Line Seyfert 1 galaxies (NLS1s, Osterbrock & Pogge (1985); Goodrich (1989)). They turned out to be the class of AGN with the steepest X-ray spectra (e.g. Puchnarewicz et al. 1992; Boller et al. 1996; Grupe 1996; Grupe et al. 1998a; Grupe et al. 2001a; Vaughan et al. 2001; Grupe et al. 2004a; Williams et al. 2002) and often show very strong X-ray variability (e.g. Boller et al. 1996; Nandra et al. 1997; Leighly 1999a; Turner et al. 1999; Grupe et al. 2001a). NLS1s are AGN with extreme properties which seem to be linked to each other: An increase in their X-ray spectral index α_X correlates with the strength of the optical FeII emission and anti-correlates with the widths of the Broad Line Region (BLR) Balmer lines and the strength of the Narrow-Line Region (NLR) forbidden lines (e.g. Grupe (1996); Grupe et al. (1999); Grupe (2004); Laor et al. (1994, 1997); Sulentic et al. (2000)). All these relationships are governed by a set of fundamental underlying parameters, usually called the Boroson & Green (1992) 'Eigenvector-1' relation in AGN. The most accepted explanation for these Eigenvectors is the Eddington ratio L/L_{Edd} or the mass of the central black hole M_{BH} (Boroson 2002; Sulentic et al. 2000; Grupe 2004; Yuan & Wills 2003) in which NLS1s are AGN with the highest Eddington ratios and smallest black hole masses for a given luminosity. The Eddington ratio has also been found to be correlated with the X-ray spectral slope α_X (Grupe 2004). Alternatively, this can also be interpreted as the age of an AGN

in which NLS1s are AGN in an early stage of their development (Grupe 1996; Grupe 2004; Mathur 2000).

RX J0148.3-2758 ($\alpha_{2000}=01^{\circ}48^{\prime}22.3$, $\delta_{2000}=-27^{\circ}58^{\prime}26^{\prime\prime}$, $z=0.121$) was discovered during the RASS as a bright and variable X-ray source (Grupe et al. 1998a; Thomas et al. 1998; Schwope et al. 2000). It was identified as a NLS1 by Grupe (1996); Grupe et al. (1999). Besides a later 6.7 ks ROSAT PSPC observation (Grupe et al. 2001a), RX J0148.3-2758 was also observed for 34 ks by ASCA (Turner et al. 1999; Vaughan et al. 1999). The 2-10 keV ASCA light curve shows that the source is highly variable (Turner et al. 1999). Its 2-10 keV spectral slope $\alpha_{2-10\text{ keV}}=0.99\pm0.17$ is typical for a Seyfert 1 galaxy (Vaughan et al. 1999). In this paper we present our observations of RX J0148.3-2758 with *Swift* which we compare with the data previously taken by ROSAT and ASCA. RX J0148.3-2758 was one of the most X-ray variable AGN in the soft X-ray selected AGN sample of Grupe et al. (2001a).

The outline of this paper is as follows: in §2 we describe the *Swift*, ROSAT and ASCA observations and the data reduction, in §3 we present the results of the *Swift* data analysis, and in §4 we discuss the results. Throughout the paper spectral indexes are denoted as energy spectral indexes with $F_{\nu} \propto \nu^{-\alpha}$. Luminosities are calculated assuming a Λ CDM cosmology with $\Omega_M=0.27$, $\Omega_{\Lambda}=0.73$ and a Hubble constant of $H_0=75 \text{ km s}^{-1} \text{ Mpc}^{-1}$ using the luminosity distances given by Hogg (1999). All errors are 1σ unless stated otherwise.

2. Observations and data reduction

RX J0148.3-2758 was observed by *Swift* between 2005-May-05 and 2005-May-13 (segments 002-006) for a total of 41575s and between 2005-December-07 and 2005-December-21 for 15,8 ks (segments 008-011). Table 1 lists the segment numbers of the *Swift* observations, the start and end times, the total observing times and the 0.2-2.0 keV rest-frame luminosities. All XRT observations were performed in PC mode. The event files were created with the standard Swift XRT analysis task *xrtpipeline* version 0.9.9. Source counts for spectra and light curves were extracted from a circle with a radius of $50''$ and the back-

ground photons in a circle near by with a radius of $100''$ between 0.3-10.0 keV. We created source and background spectra and event files using *XSELECT* version 2.3. Background subtracted light curves were created by using ESO's Munich Image Data Analysis System MIDAS version 04Sep as described in Nousek et al. (2006). The data were binned to have 250 source + background photons per bin except for the 2005 December 07 observation where we used a binning of 150 photons per bin. Note that on 2005 May 27 the *Swift* XRT detector was hit by a micro-meteorite which caused some damages. In particular the CCD columns DETX=294 and 320 had to be turned off afterwards. While our 2005 May and the 2005 December 20/21 observations are not affected by those dead columns, the 2005 December 07 and 09 observations are in part. However, when the source was positioned on one of the dead columns a correction was made to account for the loss of photons this will have caused. The spectra were rebinned using *grppha* version 3.0.0 to have at least 20 photons per bin and analyzed using *XSPEC* 12.2.1. The Auxiliary Response files were created using the *Swift* analysis task *xrtmkarf*. We used the standard response matrix version 007 with grade selection 0 to 12. Due to the low count rate, the data were not affected by pileup.

Swift UVOT data were obtained during 2005 May 11 and 13 (segments 004 and 006), and 2005 December. The UVOT was blocked during 2005 May 05 and 07 (segments 002 and 004). Data during segments 2005 May 11 and 13 were taken with the UV grism and during 2005 December we performed UVOT photometry. Because the calibration of the UV grism is still in progress and we require well-calibrated UV grism data, we do not present these data at this point. Therefore in this paper we will only present the UVOT photometry results of the 2005 December observations.

Observations were taken in the three optical and three UV filters available on the UVOT with the exception of 2005 December 07 (segment 008), where no B band observations were made. This covers the wavelength range from 1700 to 6000 Å. There was a bright star ($B\sim12.0$ mag) about $10''$ from RX J0148.3-27758 that made it necessary to carry out the UVOT photometry using a $4.5''$ source extraction region, smaller than the $6''$ and $12''$ radii that are typically used for the opti-

cal and UV filters, respectively. An aperture correction was applied to account for source photon counts that lay outside of this extraction region, in the wings of the PSF. The background region was taken from an annulus around the source, off-centered by $\sim 7''$ to avoid excessive contamination from the nearby star. Source photon counts, magnitudes and fluxes were then extracted using the UVOT tool *uvotmaghist* version 1.0 for every individual exposure taken in each filter, as well as from the co-added exposures within each segment number. All UVOT magnitudes were corrected for Galactic reddening with $E_{B-V}=0.017$.

In order to be able to carry out broadband spectral fitting, source and background data files compatible with XSPEC were created from the co-added exposures from the 2005 December 09 (segment 009) observations. This was done using the tool *uvot2pha* version 1.1. This provided a single pha file per filter. The same source and background extraction regions were used as previously, and the exposure times in the pha files were altered such that the measured count rates had the aperture correction taken into account.

The field of RX J0148.3–2758 was also observed by the BAT. However, a preliminary analysis of the BAT pointed and survey data does not show a detection of the source. So far more than 100 AGN have been detected by the BAT of which the results of about 50 have been published (Markwardt et al. 2006).

RX J0148.3–2758 was observed by ROSAT with the Position Sensitive Proportional Counter (PSPC, Pfeffermann et al. 1987) three times during the RASS for a total of 504 s and for 6.7 ks in a pointed observation (Table 1). Source counts were selected in a circular region with $R=200''$. For the RASS observations background photons were taken from two circular regions with $R=400''$ in the ROSAT scan direction (for details see Belloni et al. 1994). For the pointed observation the background was estimated from a close-by circular region with $R=400''$. Spectra were rebinned to have at least a $S/N=5$ in each bin. The light curves were binned in 400s bins. The ROSAT data were processed using the EXSAS version Apr01 (Zimmermann et al. 1998).

ASCA observed RX J0148.3–2758 on 1997 November 7 for a total of 33.2 ks with its Solid-state Imaging Spectrometers (SIS) and 36.4 ks

with the Gas Image Spectrometers (GIS) of 1997-07-11 (Table 1). A standard configuration was used during the observation. The Gas Imaging Spectrometers (GISs) were operated in PH mode throughout the observation. The Solid-state Imaging Spectrometers were operated in 1-CCD Faint mode. The SIS energy gain was reprocessed using the latest calibration file (*sisph2pi_290301.fits*). We used standard criteria for reducing the *ASCA* data. For the SIS detectors, source photons were extracted from a circular region 3.5' in radius, and for the GIS detectors, the source extraction region is 5.25' in radius. In both cases, the background was drawn from source-free regions of the detectors.

In preparation for spectral fitting, the spectra were grouped so that at least 20 photons are present in each bin. It has been demonstrated that the SIS spectra suffered degradation during the mission. The SIS efficiency loss can be parameterized by adding additional absorption to the model, where the amount of additional absorption depends on the time of the observation¹. For the time of the RX J0148.3-2758, the appropriate additional column is $4.01 \times 10^{20} \text{ cm}^{-2}$. We fit the SIS0 spectrum between 0.5 and 8.0 keV, the SIS1 spectrum between 1 and 0.8 keV, and the two GIS spectra between 0.8 and 8.0 keV.

3. Results

3.1. X-rays

3.1.1. Lightcurve

The left panel of Figure 1 shows the *Swift*-XRT light curve of RX J0148.3–2758 during the 2005 May observations (segments 002–006). The middle and right panels show the observations from 2005 December 07–09 (segments 008+009) and 2005 December 20/21 (segments 010+011), respectively. The XRT count rate light curves shown in the upper panels of Figure 1 suggest that RX J0148.3–2758 is a highly variable source. In general the AGN varies between ≈ 0.1 to 0.4 count s^{-1} . The most dramatic variability can be seen in the May 2005 light curve (left panel of Figure 1). RX J0148.3–2758 doubles its count rate by a factor of 2 within 25 ks between 90–115 ks elapsed time,

¹see <http://heasarc.gsfc.nasa.gov/docs/asca/calibration/nhparam.html> for details.

followed by an immediate drop between 120–150 ks by a factor of more than 2. A similar increase in count rate was also observed during the end of the May 2005 observation in segment 006 when RX J0148.3–2758 doubled its count rate within 18 ks. The 2005 December observations show that during the December 09 observation (middle panel) RX J0148.3–2758 became significantly fainter with a count rate of about 0.18 counts s^{-1} . The AGN became even fainter by a factor of 3 when it was re-observed on 2005-December-20 (segment 010, right panel). We do not know, however, what happened during the 10 day gap between 2005 December 09 and 20. RX J0148.3–2758 could either stayed in a low state over this period, or we just caught it by chance in this low state at the end of segment 009 and the beginning of segment 010. By the end of segment 011 the count rate increased by a factor of about 4 back again to its 'normal' level within 30 ks. The observations of 2005 December 21st were discontinued at the end of segment 011 due to the trigger of GRB 051221A (Parsons et al. 2005) which superseded the RX J0148.3–2758 observation. The most impressive increase in count rate in the RX J0148.3–2758 light curve occurs about 75 ks after the start of the 2005 May observations (left panel of Figure 1). The count rate doubles in about half a day.

The hardness ratio² plots suggest some spectral variability. Overall the hardness ratios of the 2005 December 09 (segment 009) is significantly harder than during all other observations. As we will show later this hardening reflects change in the X-ray spectrum during segment 009. There seem to be two trends present in the May 2005 light curve (left panel): a) an overall long term trend that the source becomes softer from the beginning to the end of the *Swift* coverage of about a week, and b) a short-term trend where the AGN becomes harder when RX J0148.3–2758 becomes brighter and softer when the count rate decreases. This short-term behavior has been seen in other NLS1s (e.g. RX J0134.2-4258 and RX J2217.9-5941; Grupe et al. 2000, 2001b, 2004b) the trend found in RX J0148.3-2758 is only marginal. While the hardness ratios of the December 07 and 20/21

²The hardness ratio is defined by (hard-soft)/(hard+soft) with *soft* are the count in the 0.3–1.0 keV band and *hard* in the 1.0–10.0 keV band.

observations are similar to the ones measured during May 2005, the hardness ratio of the December 09 observations is significantly harder, suggesting a change in the X-ray spectrum.

The left panel of Figure 2 shows the RASS light curves and the right panel displays the pointed ROSAT PSPC observation light curve. In both light curves RX J0148.3–2758 displays a similar variability as in the *Swift*-XRT light curve (Figure 1). RX J0148.3–2758 was one of the most variable AGN in the soft X-ray selected AGN sample of Grupe et al. (2001a).

RX J0148.3–2758 was also observed by ASCA for a period of about 1 day. Light curves were extracted in the 0.5–10 keV band for SIS detectors, and 0.8–10 keV band for the GIS detectors. The average net source count rates were 0.054, 0.043, 0.022, and 0.028 counts s^{-1} in the SIS0, SIS1, GIS2, and GIS3 detectors, respectively. The background fraction in the source regions are estimated to be 20%, 22%, 36% and 30% in the SIS0, SIS1, GIS2, and GIS3 detectors, respectively. The SIS0+SIS1 net count rate light curve, binned by orbit, is displayed in Figure 3. The light curve shows that RX J0148.3–2758 is variable by a factor of about 2. As a matter of fact, RX J0148.3–2758 was one of the AGNs with the largest excess variance (e.g. Nandra et al. 1997) found among AGNs observed by ASCA (Turner et al. 1999).

The long term light curve shown in Figure 4 displays all X-ray observation ever performed on RX J0148.3–2758. The light curve shows that during the ASCA observation RX J0148.3–2758 was in a low state – about 9 times fainter than during the RASS observation in December 1990. During the *Swift* observation in May 2005 the AGN was a factor of about 2 brighter than during the ASCA coverage, but still a factor of about 5 fainter than during the RASS. The luminosities were derived from the spectral fits described in §3.1.2.

3.1.2. Spectral Analysis

Figure 5 displays the spectra of the 2005-May (left panel) and the 2005-December (right panel) observations. All spectra were initially fitted by a single absorbed power law with the absorption column density at $z=0$ fixed to the Galactic value ($1.50 \times 10^{20} \text{ cm}^{-2}$, Dickey & Lockman (1990)). This spectral model does not result in accept-

able fits (Table 2). All spectra require multi-component spectral models such as blackbody plus power law or a broken power law model, and an additional absorption component above the Galactic column density, except for the 2005 December 09. A broken power law model as well as a blackbody plus power law model yield similar χ^2/ν and we cannot distinguish between the models. Using a blackbody model over a hard power law component yields a temperature $kT \approx 100\text{-}120$ eV which is typical for a NLS1 and agrees with the value $kT=120$ eV found by ASCA (Table 3). A broken power law model simultaneously fitted to the 2005 May XRT spectra results in a soft X-ray spectral slope $\alpha_{X,\text{soft}}=2.58^{+0.15}_{-0.12}$ which is in good agreement with the results found by ROSAT (RASS as well as pointed observation; Table 3). The XRT hard X-ray spectral slope $\alpha_{X,\text{hard}}=0.96^{+0.16}_{-0.14}$ is also in good agreement with the hard X-ray spectral slope from the ASCA data (Table 3). Alternatively to the phenomenological models we also fitted the partial covering absorber model *pcfabs*, 'warm', ionized absorber model *absori*, reflection model *pexrav*, and the disk blackbody model to the 2005 May spectra. While the *absori* and *disk blackbody* models do not show any contributions over a simple powerlaw model and the parameters of the reflection model *pexrav* could not be constraint, the partial covering model *pcfabs* yields reasonable results. We found that the 2005 May spectra can be fitted with a partial covering absorber with a column density $N_{\text{H}}=7.2^{+1.7}_{-1.3} \times 10^{22}$ cm $^{-2}$, a covering fraction $f = 0.80^{+0.03}_{-0.04}$, spectral index $\alpha_X=2.33 \pm 0.09$ with $\chi^2/\nu=428/302$ which is significantly better than a single power law fit as listed in Table 2.

The 2005 December data show some interesting spectral variability. The 2005 December 07 spectra are not well constrained due to the small number of photons (290 in 822 s). Nevertheless, the hardness ratio light curve (lower right panel of Figure 1) suggests that RX J0148.3–2758 had a similar spectrum as during the 2005 May and 2005 December 20/21 observations. However, the 6.3 ks observation from 2005 December 09 suggests that the intrinsic absorption has been vanished and the absorption column density using a single absorber at $z=0$ is consistent with just the Galactic value. In addition, using an absorbed broken power law model the soft X-ray

spectral slope $\alpha_{X,\text{soft}}=1.93^{+0.58}_{-0.42}$ is flatter than during the 2005-May observations. In order to examine this spectral change we requested a Target-of-Opportunity observation with Swift which was executed 2005 December 20/21. The spectral analysis of these data shows that RX J0148.3–2758 has become intrinsically absorbed again with $N_{\text{H,intr}} = 11.6^{+7.5}_{-5.7} \times 10^{20}$ cm $^{-2}$. Also the soft X-ray spectral slope $\alpha_{X,\text{soft}}=3.41^{+0.78}_{-0.64}$ has become significantly steeper. It is also interesting to mention that the break energy of the broken power law model fits has shifted towards softer energies between the 2005 May and December observations. During the 2005 May observations the break energy was at $E_{\text{break}} = 1.68^{+0.12}_{-0.14}$ keV while during the 2005 December observations the break energy shifted to $E_{\text{break}} \approx 1.2$ keV which agrees with the break energy $E_{\text{break}}=1.36^{+0.16}_{-0.19}$ found by ASCA when RX J0148.3–2758 was also in a low state. Due to the low number of photons in the December 09 observation the parameters of a partial covering absorber can not be constraint when all parameters are left free. However, when fixing the spectral index to the value during the 2005 May observations, $\alpha_X=2.33$, the fit results in a partial covering absorber with essentially the same covering fraction $f=0.75^{+0.06}_{-0.09}$ as during the 2005 May observation, but with a significantly lower $N_{\text{H}}=1.9^{+1.7}_{-0.9} \times 10^{22}$ cm $^{-2}$ with $\chi^2/\nu=35/35$. A partial covering absorber to the December 20/21 data increases the absorption column of the partial covering absorber to $N_{\text{H}}=3.6^{+3.2}_{-1.4} \times 10^{22}$ cm $^{-2}$, a covering fraction $f = 0.87^{+0.06}_{-0.12}$ and $\alpha_X=3.98^{+0.48}_{-0.44}$ with $\chi^2/\nu=30/27$.

The left panel of Figure 6 displays the spectra of the merged data sets of the 2005 May observations, the data set from 2005 December 09, and the merged data set from December 20/21. The right panel shows the corresponding contour plots between the intrinsic column density and the photon index $\Gamma = \alpha_X + 1$, showing no overlaps between the 2005-May, 2005 December 09, and 2005 December 20/21 observations, suggesting significant spectral variability in RX J0148.3–2758. The spectra in the left panel of Figure 6 show how the spectra change: compared with the 2005 May observations, the spectrum from December 09 has a similar hard X-ray flux, but a significantly lower flux in the soft X-ray component. Then in the December 20/21 observations the soft X-ray compo-

ment remained at a similar level as the December 09 observation. The hard X-ray flux, however, decreased by a factor of 4. By the end of the December 21st observation RX J0148.3–2758 increased its 0.3–10.0 observed flux by a factor of 3 (Figure 1).

The short-term variability we observed in RX J0148.3–2758 during the *Swift* observations seem to reflect the previous measurements by ROSAT and ASCA. During the high state observations during the RASS and ROSAT pointed observations the soft X-ray spectral slope was steep with $\alpha_{X,soft}=2.62$ and 2.25, respectively. For the spectral analysis of the ASCA data, we first constrain the power law index by fitting the region between 2 and 5 keV with a power law model. We obtain a good fit ($\chi^2 = 158$ for 173 degrees of freedom) and measure the energy index to be $1.16^{+0.27}_{-0.26}$. Next, we include the photons between 5 and 8 keV. The residuals show a slight excess that may indicate the presence of a reprocessing component. Indeed, when we plot the spectrum in this bandpass, we find the photon index flattens to 2.01, although the difference is not significant. We add a narrow iron line at 6.4 keV, but find no significant decrease in χ^2 ($\Delta\chi^2 = 1.78$). Allowing the line energy to be free finds a better fit at $6.70^{+0.18}_{-0.24}$ keV, and a larger decrease in χ^2 , although the line equivalent width is very large (550 eV), and the change in χ^2 of 5.9 compared with the no-line model shows that the improvement in fit is not significant according to the F-test. Allowing the line to be broad does not improve the fit significantly, and produces a line with unphysically large equivalent width. We conclude that evidence for a line in these data is weak, most likely because of the low signal-to-noise ratio at high energies in the spectrum. Since there is some flattening that distorts the powerlaw, we ignore the spectra above 5 keV henceforth. Note that due to the lower effective area in the *Swift* XRT at 6 keV we were not able to identify the line with the XRT.

Next, we examine the spectrum at low energies. Extrapolating down to the lower limits described above, we find that the continuum sub-tly steepens toward low energies. Indeed, fitting between 1 and 5 keV gives an energy index of 1.25 ± 0.10 , while fitting down to the lowest limits on the spectrum yields $1.48^{+0.09}_{-0.08}$. We conclude

that there is a weak soft excess present. We can model the soft excess with either a blackbody or broken power law. The fit parameters between 0.5 and 5 keV are given in Table 3. The soft X-ray spectral slope $\alpha_{X,soft}=2.03^{+0.23}_{-0.20}$ is in good agreement $\alpha_{X,soft}=1.93^{+0.58}_{-0.42}$ found during the 2005 December 09 observation by *Swift*.

3.2. UVOT Photometry

Table 4 summarizes the results of the analysis of the photometry of the co-added UVOT images. During segment 008 RX J0148.3–2758 was not observed in the B filter. Figure 7 displays the UVOT light curves of all 6 filters plus the XRT light curve from segments 008 to 011. The figure might suggest that there is some variability in the UV. However a comparison with 4 field stars as listed in Table 5 shows that the variation seen in the RX J0148.3–2758 UVOT light curves are still within the error margins. Figure 8 displays the UVOT V image of the field around RX J0148.3–2758 with the 4 comparison stars marked. In part the variations seen in the UV light curves of RX J0148.3–2758 are due to the relatively small extraction radius of 4.5" and the variable PSF of the UVOT. Therefore we conclude that RX J0148.3–2758 is not variable at optical/UV wavelengths at least not during 2005 December. However, because we do not have photometry data from the 2005 May observations we do not know what the UV flux/magnitudes are during a high-state.

3.3. Spectral Energy Distribution

Figure 9 displays the Spectral Energy Distribution (SED) of RX J0148.3–2758. For the *Swift* XRT data the 2005 May data are shown as triangles and the 2005 December 20/21 data as diagonal crosses. For the UVOT data only the 2005 December data are shown. This AGN was not detected in the NVSS or the FIRST radio catalogues. The Far-Infrared IRAS and NIR 2MASS luminosities were derived with the *GATOR* catalogue search engine at NASA/IPAC (irsa.ipac.caltech.edu/applications/Gator/). The IRAS luminosities deviate slightly from those given in Grupe et al. (1998a) due to the improved extraction software at IPAC.

From the SED plot Figure 9 we measured the

optical-to-X-ray spectral slopes α_{ox} ³ of the 2005 December 09 and 20/21 observations. During the December 09 observation we found a rest-frame $\alpha_{\text{ox}}=1.53$. With a luminosity density $\log l_o=22.78$ [W Hz⁻¹] and redshift $z=0.121$ this value is in good agreement with the mean of radio-quiet AGN ROSAT sample of Yuan et al. (1998a,b) and Strateva et al. (2005) for the same redshift and luminosity intervals. Following the relation given in equation (4) in Strateva et al. (2005), we would expect a $\alpha_{\text{ox}}=1.42$. However, during the December 20/21 observation the source became more X-ray quieted with an $\alpha_{\text{ox}}=1.81$. We have not analyzed the grism data of the May 2005 observations yet when the source was in a high state. Therefore we did not measure an α_{ox} during that time period. Even though during the 2005 December observations the UVOT data do not show significant variability, we cannot use these data for an α_{ox} measurement for the 2005 May observation, because we do not know what the flux in the UV filters was during that time period.

This NLS1 has been observed once before in the UV, in 1992 by IUE (SWP 45107). The spectrum is displayed in the left panel of Figure 10. The right panel of Figure 10 shows the optical spectrum of RX J0148.3–2758 taken in September 1995 at the ESO 1.52m telescope in La Silla for a total of 4 hours. Details of this observing run are given in Grupe et al. (2004a). With a $\text{FWHM}(\text{H}\beta)=1030\pm100$ km s⁻¹ we derived a mass of the central black hole of $1.3\times10^7 M_\odot$ using equation (5) in Vestergaard & Peterson (2006). From the IUE spectrum shown in Figure 10 we derived a $\text{FWHM}(\text{CIV})=2300$ km s⁻¹. By using the relation given in equation (7) in Vestergaard & Peterson (2006) we estimated the black hole mass $M_{\text{BH}}=3.4\times10^7 M_\odot$. Within the uncertainties both black hole masses agree with each other.

The [OIII] lines can be separated into a narrow and a blueshifted broad component. The broad [OIII] lines are blueshifted by 600 ± 200 km s⁻¹ with respect to the narrow [OIII] and H β lines. Similar results on NLS1s have been previously reported by e.g. Grupe & Leighly (2002); Zamanov et al. (2002); Aoki et al. (2005) and Bian et al. (2005).

³The X-ray loudness is defined by Tananbaum et al. (1979) as $\alpha_{\text{ox}}=-0.384 \log(f_{2\text{keV}}/f_{2500\text{\AA}})$.

4. Discussion

We presented the *Swift* observations of the highly variable NLS1 RX J0148.3–2758. Our main result, besides the strong X-ray flux variability, are the spectral changes. In RX J0148.3–2758 we observed both first a hardening of the spectrum when the X-ray flux decreased, followed by a softening while the X-ray flux was still decreasing. Both types of spectral changes have been observed in AGN. The hardening of an AGN with decreasing flux is the more typical behavior (e.g. Gallo et al. 2004a; Dewangan et al. 2002; Lee et al. 2001; Chiang et al. 2000). However, the softening on the other hand has also been reported on NLS1s, e.g. RX J2217.9–5941 (Grupe et al. 2004b), RX J0134.2–4258 (Grupe et al. 2000; Komossa & Meerschweinchen 2000), PKS 0558–504 (Gliozzi et al. 2001), and 1H 0707–495 (Gallo et al. 2004b; Fabian et al. 2004).

The easiest way to produce a hardening with decreasing observed X-ray flux is having a cold absorber cloud passing the line of sight. Variable absorber in AGN are often observed in Seyfert galaxies, e.g. the Seyfert 2 sample of Risaliti et al. (2002), NGC 1365 (Risaliti et al. 2004), NGC 4388 (Elvis et al. 2004), the Seyfert 1.8 galaxy NGC 3786 Komossa & Fink (1997b) the Seyfert 1.5 galaxies NGC 4151 (Puccetti et al. 2004) and NGC 3227 Komossa & Fink (1997a), or 1H0419–577 (Pounds et al. 2004). Also for RX J0148.3–2758, a variable cold absorber is, at least in part, a plausible explanation for the spectral variability between the 2005 May and 2005 December 09 observation. As listed in Table 2 we fitted and absorbed broken power law to the 2005 December 09 data by fixing the broken power law parameters to those found in May 2005 and allowing only the absorption column density and the normalization to vary. The result is that we can fit the data with a column density $N_{\text{H}}=8.1\pm1.4\times10^{20}$ cm⁻². The fit shows, however, strong residuals below 0.5 keV. Even though NLS1s are often seen as AGN with only minor intrinsic absorption, this picture is not true in general (e.g. Grupe et al. 1998b, 2004c). This is not the result, however, when leaving all parameters free. As listed in Table 2 and shown in Figure 6 the N_{H} actually becomes consistent with the Galactic value and the the soft X-ray spectral index $\alpha_{\text{X,soft}}$ flattens. However, in a fitting rou-

tine like *XSPEC* N_{H} and the spectral index are not independent of each other. A larger value of the absorption column density N_{H} will result in a steeper spectral index, and vice-versa. Especially considering that the December 20/21 observation show a column density in the order of 10^{21} cm^{-2} again, we can conclude that the spectral change seen between the 2005 May and 2005 December 09 observations is most likely due to an increase in the absorber column density. A soft X-ray spectrum fitted by a spectral model can mimic a low column density as shown by e.g. Puchnarewicz et al. (1995) and Grupe et al. (1998a), even though the real column density is much larger.

A softening with decreasing X-ray flux can be caused by several processes. Gliozzi et al. (2001) explained the spectral variability seen in radio-loud AGN PKS 0558–504 by the presence of a jet, however this model does not apply for RX J0148.3–2758, which is radio-quiet. In the case of RX J0134.2–4258, Grupe et al. (2000) explained this behavior by a change in the accretion disk corona, while Komossa & Meerschweinchen (2000) argues for a variable ionized absorber. However, our *Swift* XRT spectra of RX J0148.3–2758 do not suggest the presence of a simple one-component warm absorber. Another possibility is the presence of a partial covering absorber as discussed for e.g. RX J2217.9–5941 (Grupe et al. 2004b), 1H 0707–495 (Gallo et al. 2004b; Tanaka et al. 2004), and Mkn 1239 (Grupe et al. 2004c). As an alternative, Fabian et al. (2004) discussed the variability in 1H 0707–495 in the context of X-ray reflection on an ionized disk. From all these models, only the partial covering absorber model yields reasonable results. Interestingly, the coverage fraction of the 2005 May, 2005 December 09, and December 20/21 observation is always the same at around $f=0.8$. The column density of the partial covering absorber follows the same trend as the cold absorber column density, which means it seems to be at a low value during the December 09 observation.

The soft X-ray slope $\alpha_{\text{X,soft}}=2.58^{+0.15}_{-0.12}$ is rather steep even for a NLS1. The mean soft X-ray slope of the 51 NLS1s of the sample of Grupe et al. (2004a) is $\alpha_{\text{X}}=1.96$ with a standard deviation $\sigma=0.41$, and $\alpha_{\text{X}}=2.1$ from the sample of Boller et al. (1996). However, its hard X-ray spectral slope $\alpha_{\text{X}}=0.96^{+0.16}_{-0.12}$ is slightly flatter than what has been

found in the NLS1s sample of Leighly (1999b) who a mean hard X-ray slope of $\alpha_{\text{X}}=1.19\pm0.10$ and Brandt et al. (1997) with $\alpha_{\text{X}}=1.15$. This is closer to the values found for BLS1 for which Leighly (1999b) found $\alpha_{\text{X}}=0.78\pm0.11$ and Brandt et al. (1997) with $\alpha_{\text{X}}=0.87$. There can be one explanation for this ‘discrepancy’: while the soft X-ray spectral slope is driven by the Eddington ration L/L_{Edd} , the hard X-ray spectral slope is more dependent on the black hole mass. With an Eddington ration $L/L_{\text{Edd}}=4$ it is one of the NLS1s with the highest L/L_{Edd} in the sample of Grupe et al. (2004a).

High Eddington accretion objects like NLS1s are also thought to be sources with strong outflows (e.g. King & Pounds 2003; Pounds et al. 2003). Arguing for this is out finding of a strong blueshift in the [OIII] lines in RX J0148.3–2758 (Grupe & Leighly 2002). It has been found in general that NLS1s show strong blueshift of the [OIII] emission lines (e.g. Zamanov et al. 2002; Bian et al. 2005; Aoki et al. 2005) suggesting strong outflows.

From nearby galaxies it has been found that there is a relatively tight relation between the mass of the central black hole M_{BH} and the bulge stellar velocity dispersion σ (e.g. Gebhardt et al. 2000a; Ferrarese & Merritt 2000; Tremaine et al. 2003). This relation for normal galaxies also extends to active galaxies (Gebhardt et al. 2000b; Ferrarese et al. 2001). Based on the results by Nelson & Whittle (1995) and Nelson & Whittle (1996), Nelson (2000) suggested to use the FWHM([OIII]) as a surrogate for the stellar velocity dispersion σ . As shown by Grupe & Mathur (2004); Mathur & Grupe (2005a,b), NLS1s with a high Eddington ratio L/L_{Edd} deviate significantly from the $M_{\text{BH}} - \sigma$ relation. With a $\text{FWHM}(\text{[OIII]})=700\pm500$ and a black hole mass in the order of a few $10^7 M_{\odot}$ RX J0148.3–2758 is one of the most extreme cases that deviate from the Tremaine et al. (2003) $M_{\text{BH}} - \sigma$.

Our *Swift* observations of RX J0148.3–2758 can also explain the large scatter in the α_{ox} diagrams of Yuan et al. (1998a,b) and Strateva et al. (2005). While during the 2005 December 09 observation we measured $\alpha_{\text{ox}}=1.5$, RX J0148.3–2758 became X-ray weak with $\alpha_{\text{ox}}=1.81$ during the December 20/21 observations. This strong change in α_{ox} suggest that the X-ray weakness observed in some NLS1s, e.g. in the SDSS NLS1 sample

of Williams et al. (2002, 2004) is most likely of temporary nature. Part of the X-ray weakness reported by Brandt et al. (2000) for Palomar-Green AGN of the Boroson & Green (1992) sample can also be explained by our observations. As Brandt et al. (2000) suggested, the X-ray weakness found in the sources of their sample is most likely caused by absorption rather than an intrinsic nature. However, as we have seen too in RX J0148.3–2758, we also noticed a change in the hard X-ray component which does not affect the emission at soft X-ray energies and in the optical/UV either. When the hard X-ray spectrum changed we did not detect any significant change in the UV filters.

The *Swift* observations of RX J0148.3–2758 have shown the great potential of *Swift* for AGN science. The X-ray light curves of AGN in particular NLS1s are highly variable and need a long coverage at multi-wavelengths. Due to its low-earth orbit, *Swift* is very similar to ROSAT and ASCA, but also has the advantage of being a multi-wavelength observatory with its UVOT, XRT and BAT instruments. Our study has also shown how important the simultaneous UV and X-ray observations over a time-span of days are. *Swift* is the only observatory that can obtain this type of observations. Our observations of RX J0148.3–2758 took advantage of the multi-wavelength capacity as well as the flexible scheduling of *Swift*. The simultaneous observations in the UVOT and XRT allow us to measure the X-ray loudness α_{ox} directly without assuming any optical/UV spectral slopes. We are also able to measure the total power in the Big Blue Bump and therefore the bolometric luminosity directly. With the strong change in its spectrum between the 2005 May and 2005 December 09 observations we requested a Target-of-Opportunity observation with *Swift* which was approved and executed a few days later on December 20/21. This additional observation allowed us to observe a hardening and a softening in the same source. Based on this interesting spectral behavior, we plan to continue observing RX J0148.3–2758 with *Swift*.

We would like to thank the whole *Swift*-team for making this observation possible, especially the *Swift* science planners Jamie Kennea, Sally Hunsberger, Claudio Pagani, Judy Racusin and

Antonino Cucchiara for scheduling RX J0148.3–2758 for such a long observing time, and Neil Gehrels for approving the ToO observations of 2005-December 20/21. We would also like to thank Marco Ajello and Jochen Greiner (MPE) and Jack Tueller (GSFC) for checking the BAT pointed and survey data for any detection of RX J0148.3–2758. This research has made use of the NASA/IPAC Extra-galactic Database (NED) which is operated by the Jet Propulsion Laboratory, Caltech, under contract with the National Aeronautics and Space Administration. This research was supported by NASA contract NAS5-00136 (D.G., D.B., & J.N.).

REFERENCES

Aoki, K., Kawaguchi, T., & Ohta, K., 2005, ApJ, 618, 601

Barthelmy, S.D., 2005, Space Science Reviews, 120, 143

Belloni, T., Hasinger, G., & Izzo, C., 1994, A&A, 283, 1037

Beuermann, K., Thomas, H.-C., Reinsch, K., et al., 1999, A&A, 347, 47

Bian, W., Yuan, Q., & Zhao, Y., 2005, MNRAS, 364, 187

Boller, T., Brandt, W.N., & Fink, H.H., 1996, A&A, 305, 53

Boroson, T.A., & Green, R.F., 1992, ApJS, 80, 109

Boroson, T.A., 2002, ApJ, 565, 78

Brandt, W.N., Mathur, S., & Elvis, M., 1997, MNRAS, 285, L25

Brandt, W.N., Laor, A., & Wills, B.J., 2000, ApJ, 528, 637

Burrows, D., et al., 2005, Space Science Reviews, 120, 165

Chiang, J., Reynolds, C.S., Blaes, O.M., Nowak, M.A., Murray, N., Madejski, G., Marshall, H.L., & Magdziarz, P., 2000, ApJ, 292

Dewangan, G.C., Boller, Th., Singh, K.P., & Leighly, K.M., 2002, A&A, 390, 65

Dickey, J.M., & Lockman, F.J., 1990, *ARA&A*, 28, 215

Diplas, A., & Savage, B.D., 1994, *ApJ*, 427, 274

Elvis, M., Risaliti, G., Nicastro, F., Miller, J.J., Fiore, F., & Puccetti, S., 2004, *ApJ*, 615, L25

Fabian, A.C., Miniutti, G., Gallo, L.C., Boller, Th., Tanaka, Y., Vaughan, S., & Ross, R., 2004, *MNRAS*, 353, 1071

Ferrarese, L., & Merritt, D., 2000, *ApJ*, 539, L9

Ferrarese, L., Pogge, R.W., Peterson, et al., 2001, *ApJ*, 555, L55

Gallo, L.C., Boller, Th., Brandt, W.N., Fabian, A.C., & Grupe, D., 2004a, *MNRAS*, 352, 744

Gallo, L.C., Tanaka, Y., Boller, Th., Fabian, A.C., Vaughan, S., & Brandt, W.N., 2004, *MNRAS*, 353, 1064

Gebhardt, K., Bender, R., Bower, G., et al., 2000, *ApJ*, 539, L13

Gebhardt, K., Kormendy, J., Ho, L.C., et al., 2000, *ApJ*, 543, L5

Gehrels, N., et al., 2004, *ApJ*, 611, 1005

Gliozzi, M., Brinkmann, W., O'Brien, P.T., Reeves, J.N., Pounds, K.A., Trioglio, M., & Giannotti, F., 2001, *A&A*, 365, L128

Goodrich, R.W., 1989, *ApJ*, 342, 224

Grupe, D., 1996, PhD Thesis, Universität Göttingen

Grupe, D., 2004, *AJ*, 127, 1799

Grupe, D., Beuermann, K., Thomas, H.-C., Mannheim, K., & Fink, H.H., 1998, *A&A* 330, 25

Grupe, D., Wills, B.J., Wills, D., Beuermann, K., 1998, *A&A*, 333, 827

Grupe, D., Beuermann, K., Mannheim, K., & Thomas, H.-C., 1999, *A&A*, 350, 805

Grupe, D., Leighly, K.M., Thomas, H.-C., & Laurent-Muehleisen, S.A., 2000, *A&A*, 356, 11

Grupe, D., Thomas, H.-C., & Beuermann, K., 2001a, *A&A*, 367, 470

Grupe, D., Thomas, H.-C., & Leighly, K.M., 2001b, *A&A*, 369, 450

Grupe, D., & Leighly, K.M., 2002, MPE report 279, p287

Grupe, D., Wills, B.J., Leighly, K.M., & Meusinger, H., 2004a, *AJ*, 127, 156

Grupe, D., Leighly, K.M., Burwitz, V., Predehl, P., & Mathur, S., 2004b, *AJ*, 128, 1524

Grupe, D., Mathur, S., & Komossa, S., 2004c, *AJ*, 127, 3161

Grupe, D., & Mathur, S., 2004, *ApJ*, 606, L41

Hill, J.E., et al., 2004, SPIE, 5165, 217

Hogg, D., 1999, *astro-ph/9905116*

King, A.R., & Pounds, K.A., 2003, *MNRAS*, 345, 657

Komossa, S., & Fink, H.H., 1997a, *A&A*, 327, 483

Komossa, S., & Fink, H.H., 1997b, *A&A*, 327, 483

Komossa S., & Fink H., 1998, in: *Highlights in X-ray astronomy*, B. Aschenbach & M.J. Freyberg (eds.), MPE Report 272, 147

Komossa, S., & Meerschweinchen, J., 2000, *A&A*, 354, 411

Laor, A., Fiore, F., Elvis, M., Wilkes, B.J., & McDowell, J.C., 1994, *ApJ*, 435, 611

Laor, A., Fiore, F., Elvis, M., Wilkes, B.J., & McDowell, J.C., 1997, *ApJ*, 477, 93

Lee, J.C., Fabian, A.C., Reynolds, C.S., Brandt, W.N., & Iwasawa, K., 2001, *MNRAS*, 318, 857

Leighly, K.M., 1999a, *ApJS*, 125, 297

Leighly, K.M., 1999b, *ApJS*, 125, 317

Markwardt, C.B., Tueller, J., Skinner, G.K., Gehrels, N., Barthelmy, S.D., & Mushotzky, R.F., 2006, *ApJ*, submitted, *astro-ph/0509860*

Mason, K.O., et al., 2001, *A&A*, 365, L36

Mathur, S., 2000, *MNRAS*, 314, L17

Mathur, S., & Grupe, D., 2005a, *A&A*, 432, 463

Mathur, S., & Grupe, D., 2005b, *ApJ*, 633, 688

Nandra, K., George, I.M., Mushotzky, R.F., Turner, T.J., & Yaqoob, T., 1997, *ApJ*, 476, 70

Nelson, C.H., 2000, *ApJ*, 544, L91

Nelson, C.H., & Whittle, M., 1995, *ApJS*, 99, 67

Nelson, C.H., & Whittle, M., 1996, *ApJ*, 465, 96

Nousek, J.A., et al., 2006, *ApJ*, accepted, *astro-ph/0508332*

Osterbrock, D.E., & Pogge, R.W., 1985, *ApJ*, 297, 166

Parsons, A., et al. 2005, *GCN* 4363

Pfeffermann, E., Briel, U.G., Hippmann, H., et al., 1987, *SPIE*, 733, 519

Pounds, K.A., Done, C., & Osborne, J.P., 1995, *MNRAS*, 277, L5

Pounds, K.A., Reeves, J.N., King, A.R., Page, K.L., O'Brien, P.T., & Turner, M.J.L., 2003, *MNRAS*, 345, 705

Pounds, K.A., Reeves, J.N., Page, K.L., & O'Brien, P.T., 2004, *ApJ*, 616, 696

Puccetti, S., Risaliti, G., Fiore, F., Elvis, M., Nicastro, F., Perola, G.C., & Capalbi, M., 2004, *Nucl. Phys. B Suppl.*, 132, 225

Puchnarewicz, E.M., et al., 1992, *MNRAS*, 256, 589

Puchnarewicz, E.M., Mason, K.O., Siemiginowska, A., & Pounds, K.A., 1995, *MNRAS*, 276, 20

Risaliti, G., Elvis, M., & Nicastro, F., 2002, *ApJ*, 571, 234

Risaliti, G., Elvis, M., Fabbiano, G., Baldi, A., & Zezas, A., 2004, *ApJ*, 623, L93

Rodríguez-Pascual, P.M., Mas-Hesse, J.M., & Santos-Lleó, M., 1997, *A&A*, 327

Roming, P.W.A., et al., 2005, *Space Science Reviews*, 120, 95

Schwone, A.D., Hasinger, G., Lehmann, I., et al., 2000, *AN*, 321, 1

Shields, G.A., 1978, *Nature*, 272, 706

Strateva, I.V., Brandt, W.N., Schneider, D.P., Vanden Berk, D.G., & Vignali, C., 2005, *ApJ*, 130, 387

Sulentic, J.W., Zwitter, T., Marziani, P., & Dultzin-Hacyan, D., 2000, *ApJ*, 536, L5

Tanaka, Y., Boller, Th., Gallo, L.C., Keil, R., & Ueda, Y., 2004, *PASJ*, 56, L9

Tananbaum, H., et al., 1979, *ApJ*, 234, L9

Thomas, H.-C., Beuermann, K., Reinsch, K., et al., 1998, *A&A*, 335, 467

Tremaine, S., Gebhardt, K., Bender, R., et al., 2003, *ApJ*, 574, 740

Trümper, J., 1982, *Adv. Space Res.*, 4, 241

Turner, M.J.L., Abbey, A., Arnaud, M., et al., 2001, *A&A*, 365, L27

Turner, T.J., George, I.M., Nandra, K., & Turcan, D., 1999, *ApJ*, 524, 667

Vaughan, S., Reeves, J., Warwick, R., & Edelson, R., 1999, *MNRAS*, 309, 113

Vaughan, S., Edelson, R., Warwick, R.S., Malkan, M.A., & Goad, M.R., 2001, *MNRAS*, 327, 673

Vestergaard, M., & Peterson, B.M., 2006, *ApJ*, accepted, *astro-ph/0601303*

Voges, W., Aschenbach, B., Boller, T., et al., 1999, *A&A*, 349, 389

Walter, R., & Fink, H.H., 1993, *A&A*, 274, 105

Williams, R.J., Pogge, R.W., & Mathur, S., 2002, *AJ*, 124, 3042

Williams, R.J., Pogge, R.W., & Mathur, S., 2004, *ApJ*, 610, 737

Yuan, W., Brinkmann, W., Siebert, J., Voges, W., 1998a, *A&A*, 330, 108

Yuan, W., Siebert, J., & Brinkmann, W., 1998b, *A&A*, 334, 498

Yuan, M.J., & Wills, B.J., 2003, *ApJ*, 593, L11

Zamanov, R., Marziani, P., Sulentic, J.W., Galvani, M., Dultzin-Hacyan, D., & Bachev, R., 2002, ApJ, 576, L9

Zimmermann, U., Boese, G., Becker, W., et al., 1998, 'EXSAS User's Guide', MPE report (<http://wave.xray.mpe.mpg.de/exsas/users-guide>)

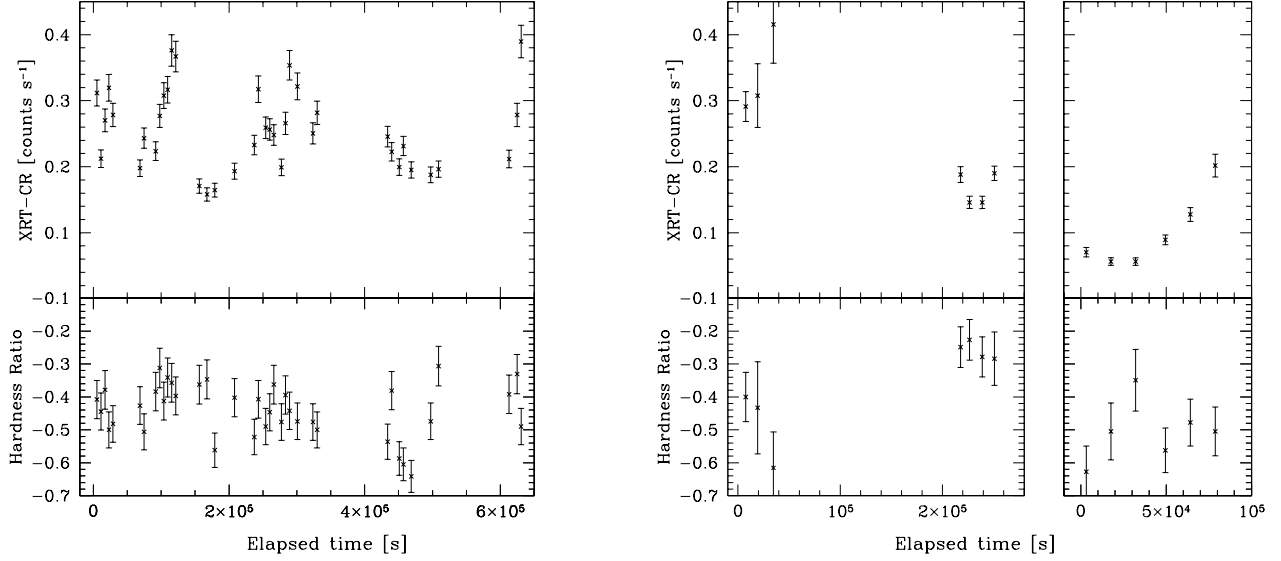


Fig. 1.— Swift XRT 0.3-10.0 keV light curve, the left panel shows the 2005 May the middle one the December 07 and 09, and the right one the December 20 and 21 observations Start times are 2005-May-06 00:05 UT, 2005-December-07 00:34 UT, and 2005-December-20 13:40 UT, for the left, middle and right panels, respectively. The start and end times of each segment are given in table 1. The upper panel displays the count rate light curve and the lower panel the light curve of the hardness ratio = $(H-S)/(H+S)$ with S and H are the number of photons in in the 0.3-1.0 and 1.0-10.0 keV band, respectively.

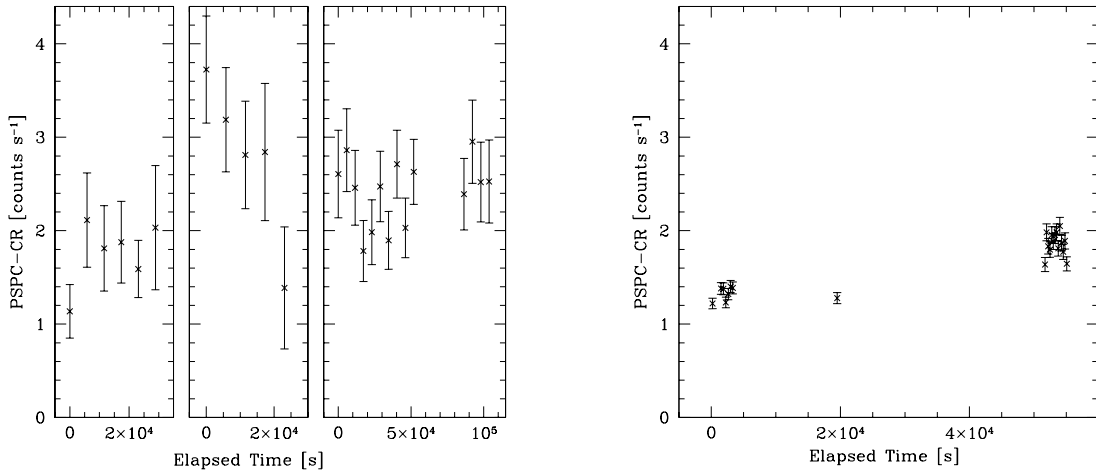


Fig. 2.— ROSAT All-Sky Survey and pointed observation light curves. The start times are 1990-07-15 15:26 UT, 1990-12-28 01:01 UT, and 1991-01-15 09:24 UT for the RASS observations (left panels), and 1992-07-09 09:54 for the pointed ROSAT PSPC observation (right panel)

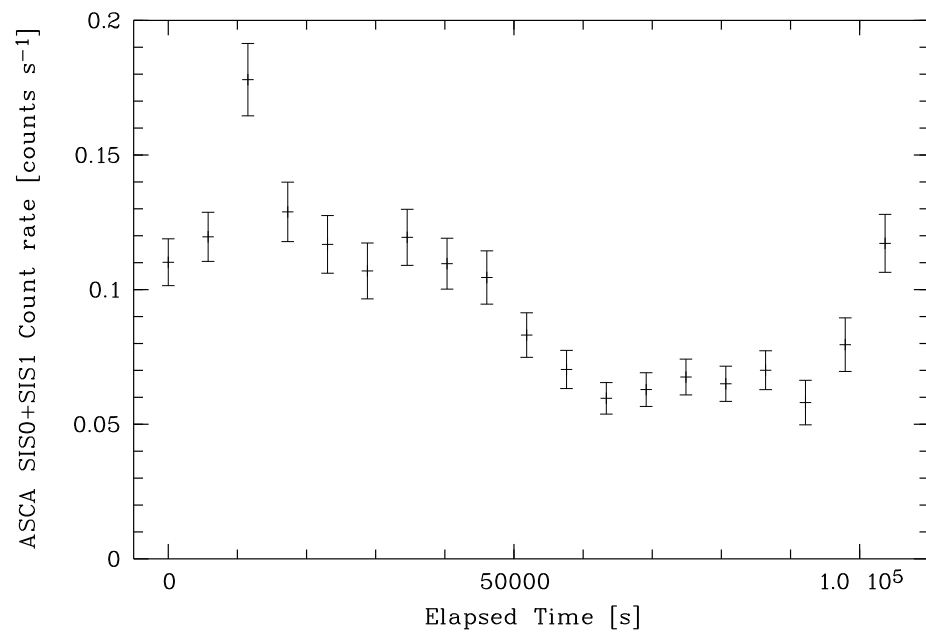


Fig. 3.— ASCA SIS0 + SIS1 light curve, Start time is 1997-July-1 21:05 UT

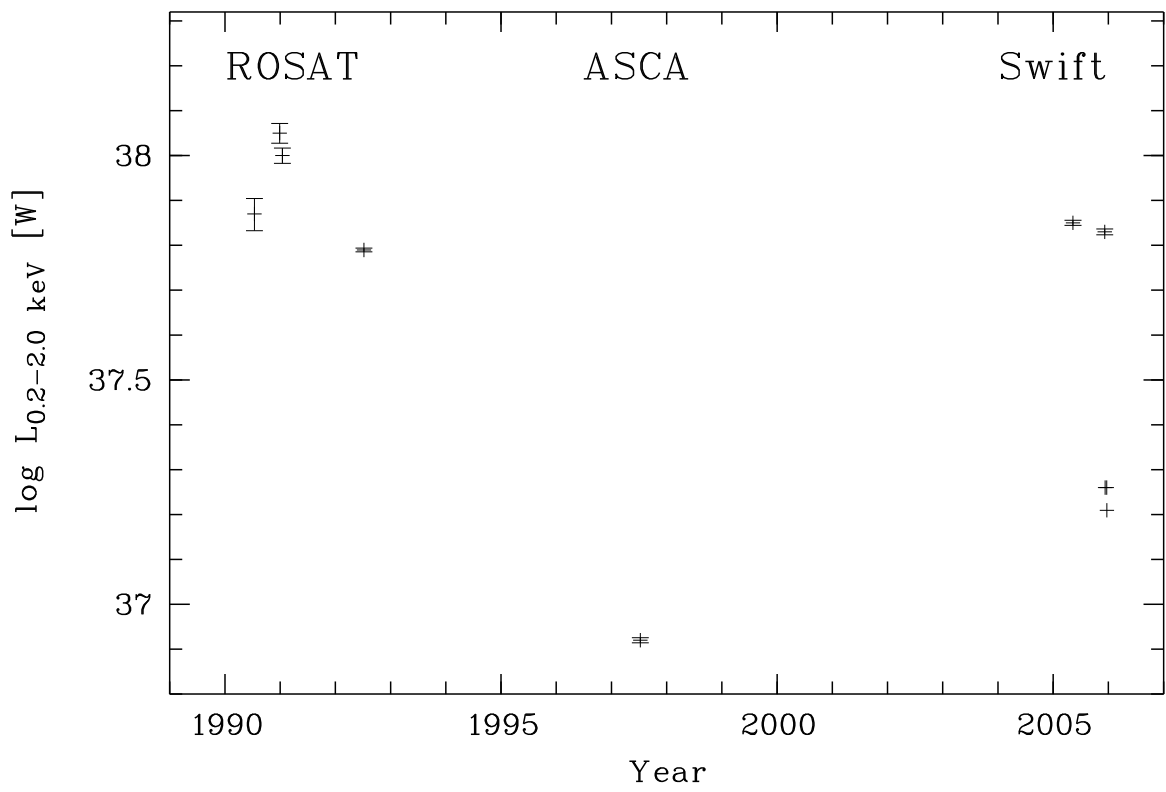


Fig. 4.— Long-term light curve of RX J0148.3–2758. The luminosities are rest-frame 0.2–2.0 keV.

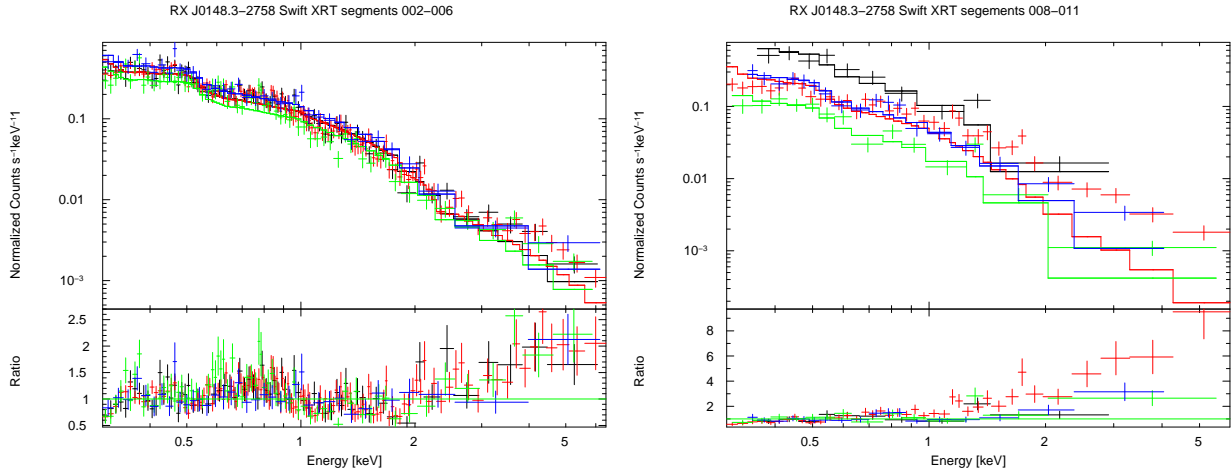


Fig. 5.— Swift XRT spectra of RX J0148.3–2758. The spectra of segments 002–006 (left panel) were fitted by a single power law with the absorption column fixed to the Galactic value. For the spectra of segments 008–011 also the X-ray spectral slope was fixed to $\alpha_X=2.4$ (see text).

RX J0148.3-2758 Swift XRT segments 002–006 (white), 009 (red), 010–011(green)

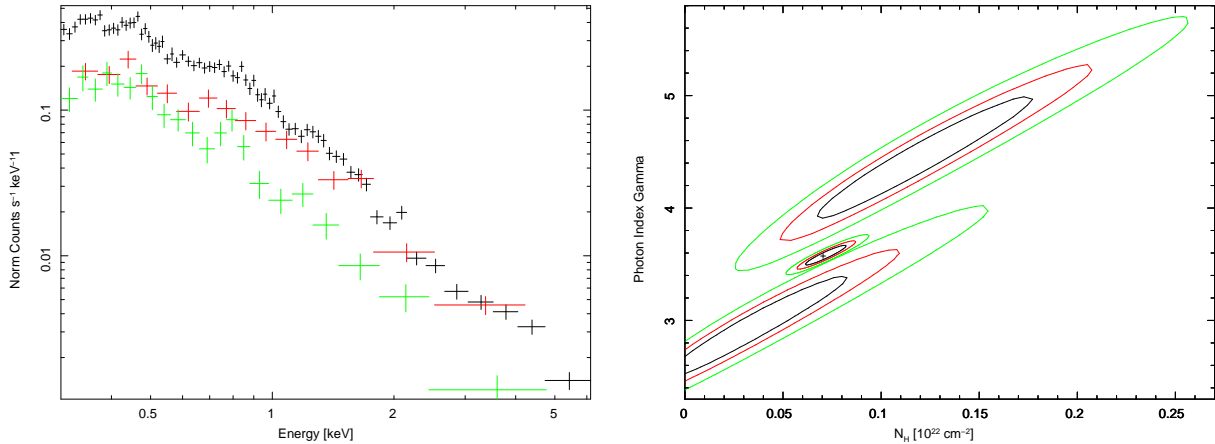


Fig. 6.— Comparison between the spectra of the 2005 May, 2005 December 09, and December 20/21 observations. The left panel displays the spectra and the right panel shows the contour plot between the intrinsic column density $N_{\text{H,intr}}$ and the soft X-ray Photon index $\Gamma = \alpha_{\text{X,soft}} + 1$ of the XRT spectra. The contour plot of the May 2005 observations is the one in the middle, the one in the lower left corner is the contour plot of the December 09 observation (segment 009) and the upper right is the December 20/21 (segments 010 + 011).

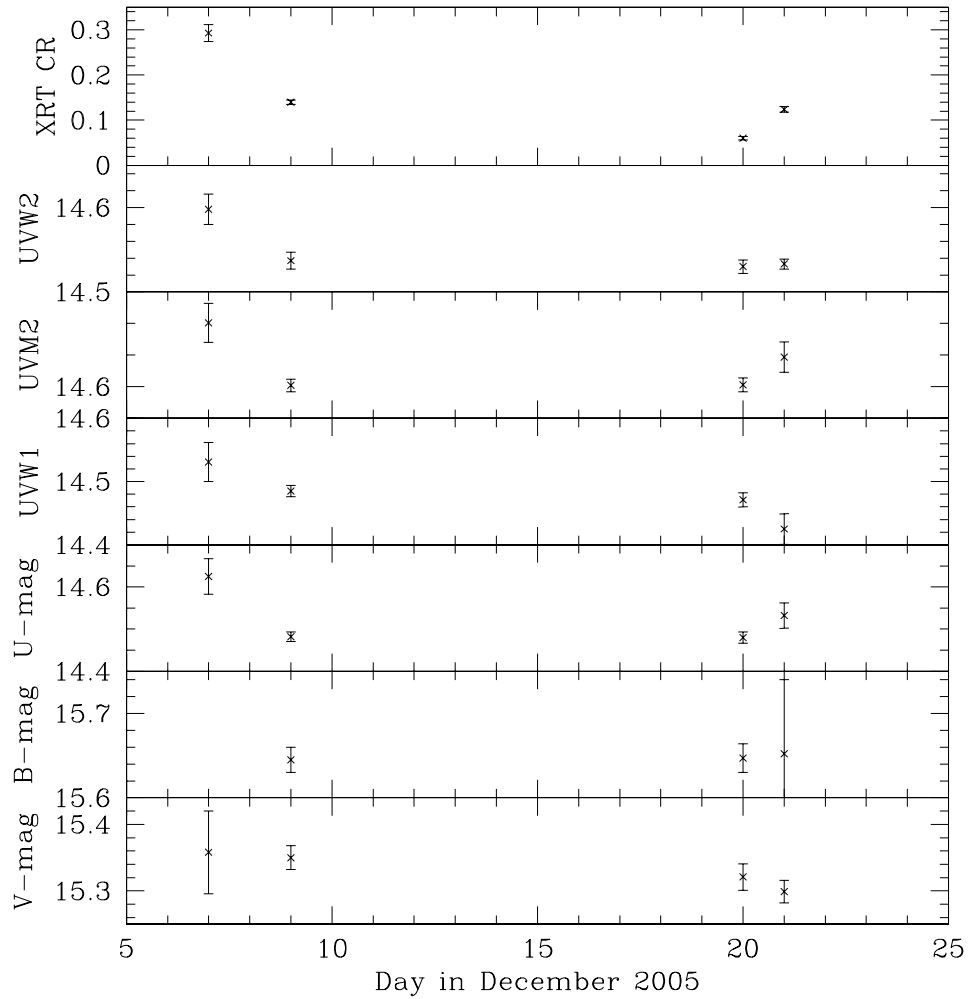


Fig. 7.— XRT and UVOT light curves.

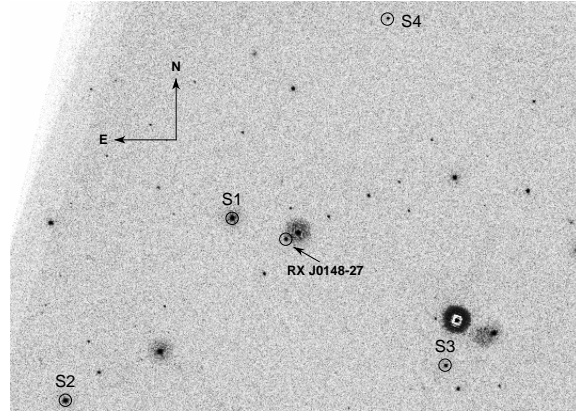


Fig. 8.— UVOT V-image of the field around RX J0148.3–2758. The 4 comparison stars as listed in Table 5 are marked as S1 - S4 in the figure.

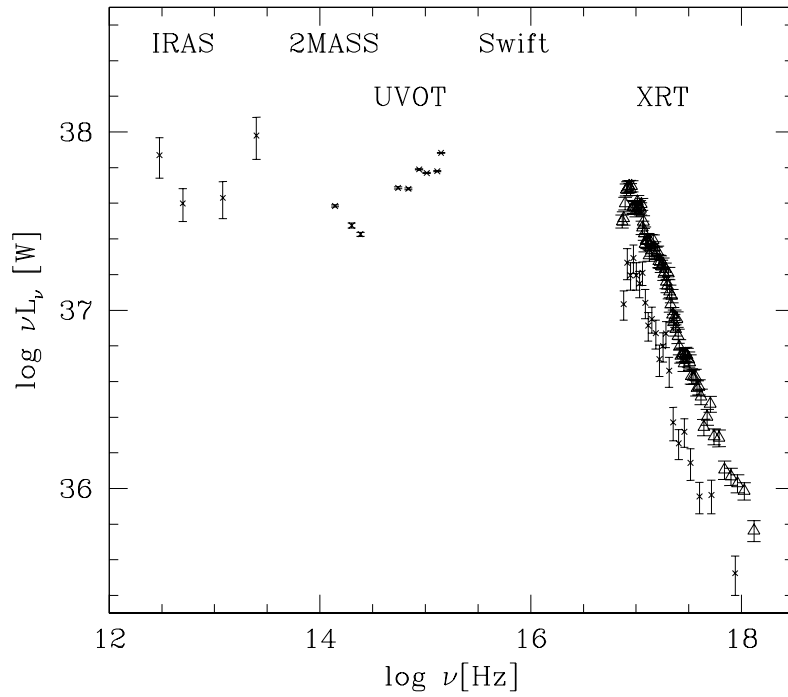


Fig. 9.— Spectral Energy Distribution of RX J0148.3–2758 The diagonal crosses of the *Swift* UVOT and XRT data represent the 2005 December 20/21 observations and the triangles the XRT observations from 2005 May.

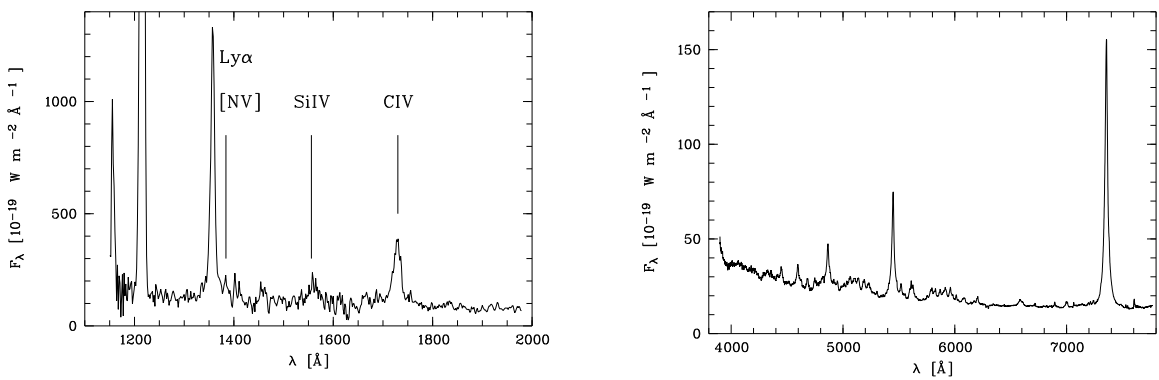


Fig. 10.— IUE and optical spectra of RX J0148.3–2758

TABLE 1
OBSERVATION LOG OF RX J0148.3–2758

Observatory	observation	T-start ¹	T-stop ¹	T _{exp} ²	log L _X ³
<i>Swift</i>	segment 002	2005-05-06 00:05	2005-05-06 24:00	7637	37.85 ⁴
	segment 003	2005-05-07 00:05	2005-05-09 22:58	21966	
	segment 004	2005-05-11 00:27	2005-05-11 23:11	8840	
	segment 006	2005-05-13 00:45	2005-05-13 10:26	3132	
	segment 008	2005-12-07 00:34	2005-12-07 10:35	822	37.83
	segment 009	2005-12-09 12:17	2005-12-09 23:54	6346	37.27
	segment 010	2005-12-20 13:40	2005-12-20 23:32	5110	37.26
	segment 011	2005-12-21 01:01	2005-12-21 14:00	3506	37.21
	SIS 0, 1	1997-07-11 21:11	1997-07-13 03:07	33243	36.92
	GIS 2, 3	1997-07-11 21:11	1997-07-13 03:07	36381	
ROSAT	pointed PSPC	1992-07-09 09:54	1992-07-10 01:16	6652	37.79
ROSAT	RASS	1990-07-15 15:26	1990-07-16 07:28	89	37.87
		1990-12-28 01:11	1990-12-29 07:37	140	38.05
		1991-01-15 09:24	1991-01-17 07:49	274	38.00

¹Start and End times are given in UT

²Observing time given in s

³0.2-2.0 keV luminosity given in units of W

⁴Average of segments 002-006

⁵Average of segments 008-009

TABLE 2

SPECTRAL PARAMETERS OF THE FITS TO THE *Swift*-XRT SPECTRA OF RX J0148.3-2758

Obs. Date	Model ¹	$N_{\text{H, Gal}}$ 10^{20} cm^{-2}	$N_{\text{H, intr}}$ 10^{20} cm^{-2}	$\alpha_{\text{X, soft}}$ ²	kT eV	E_{break} KeV	$\alpha_{\text{X, hard}}$	χ^2/ν
May 06	1	1.50 (fix)	—	1.84 \pm 0.07	—	—	—	113/68
	1	3.33 $^{+0.14}_{-0.12}$	—	2.03 $^{+0.16}_{-0.15}$	—	—	—	107/67
	1	1.50 (fix)	3.01 $^{+0.22}_{-0.19}$	2.08 $^{+0.19}_{-0.17}$	—	—	—	106/67
	2	1.50 (fix)	—	—	126 $^{+8}_{-11}$	—	1.27 $^{+0.30}_{-0.21}$	83/65
	3	4.80 \pm 1.16	—	2.28 \pm 0.14	—	1.87 \pm 0.25	0.95 \pm 0.24	83/65
	4	1.50 (fix)	7.95 $^{+0.25}_{-0.34}$	2.59 $^{+0.21}_{-0.29}$	—	1.80 $^{+0.16}_{-0.19}$	0.85 $^{+0.35}_{-0.23}$	71/64
	1	1.50 (fix)	—	1.82 \pm 0.03	—	—	—	268/130
	1	2.77 \pm 0.05	—	1.96 \pm 0.05	—	—	—	258/129
	1	1.50 (fix)	2.34 $^{+1.17}_{-1.09}$	2.02 $^{+0.11}_{-0.10}$	—	—	—	254/129
	2	1.50 (fix)	—	—	118 $^{+5}_{-7}$	—	1.23 $^{+0.14}_{-0.13}$	179/127
May 07	3	4.85 $^{+0.93}_{-0.67}$	—	2.30 $^{+0.12}_{-0.11}$	—	1.72 $^{+0.15}_{-0.16}$	1.01 $^{+0.18}_{-0.17}$	174/126
	4	1.50 (fix)	7.61 $^{+0.20}_{-0.17}$	2.61 $^{+0.19}_{-0.16}$	—	1.61 \pm 0.14	1.00 $^{+0.19}_{-0.13}$	146/126
	1	1.50 (fix)	—	1.93 \pm 0.05	—	—	—	155/67
	1	3.88 \pm 0.09	—	2.13 \pm 0.10	—	—	—	145/66
May 11	2	1.50 (fix)	—	—	120 \pm 7	—	0.87 $^{+0.14}_{-0.13}$	84/65
	3	6.18 $^{+1.81}_{-1.56}$	—	2.53 $^{+0.25}_{-0.20}$	—	1.75 $^{+0.25}_{-0.30}$	0.69 $^{+0.36}_{-0.36}$	98/63
	4	1.50 (fix)	7.88 $^{+0.36}_{-0.41}$	2.75 $^{+0.32}_{-0.41}$	—	1.70 $^{+0.33}_{-0.18}$	0.68 $^{+0.33}_{-0.32}$	92/63
	1	1.50 (fix)	—	1.83 \pm 0.10	—	—	—	27/36
May 13	1	1.60 $^{+0.17}_{-0.15}$	—	1.84 $x^{+0.20}_{-0.18}$	—	—	—	27/35
	2	1.50 (fix)	—	—	108 $^{+108}_{-102}$	—	1.64 $^{+0.25}_{-0.26}$	25/34
	3	1.50 (fix)	—	1.93 \pm 0.08	—	1.70 (fix)	1.37 \pm 0.23	23/34
	3	3.01 $^{+1.80}_{-1.60}$	—	2.10 $^{+0.21}_{-0.19}$	—	1.42 \pm 0.50	1.47 \pm 0.30	24/33
May 06-13 ³	4	1.50 (fix)	3.42 $^{+0.33}_{-0.11}$	2.24 \pm 0.16	—	1.40 $^{+1.02}_{-3.24}$	1.47 $^{+1.90}_{-3.11}$	23/32
	1	1.50 (fix)	—	1.84 \pm 0.03	—	—	—	567/304
	1	2.92 $^{+0.55}_{-0.53}$	—	2.00 \pm 0.07	—	—	—	546/303
	1	1.50 (fix)	2.42 $^{+0.86}_{-0.82}$	2.05 \pm 0.08	—	—	—	541/303
December 07	2	1.50 (fix)	—	—	119 \pm 4	—	1.23 $^{+0.04}_{-0.06}$	386/299
	3	4.96 $^{+0.68}_{-0.46}$	—	2.33 \pm 0.08	—	1.76 \pm 0.11	0.96 \pm 0.13	386/300
	4	1.50 (fix)	7.15 $^{+1.48}_{-1.21}$	2.58 $^{+0.15}_{-0.12}$	—	1.68 $^{+0.12}_{-0.14}$	0.96 $^{+0.16}_{-0.14}$	347/301
	1	1.50 (fix)	—	2.17 $^{+0.27}_{-0.25}$	—	—	—	12/7
December 09	2	1.50 (fix)	—	—	104 \pm 16	—	1.36 $^{+1.21}_{-1.36}$	10/6
	3	1.50 (fix)	—	2.26 \pm 0.32	—	1.07 \pm 1.39	1.86 \pm 0.80	11/6
	1	1.50 (fix)	—	1.48 $^{+0.10}_{-0.09}$	—	—	—	30/37
	2	1.50 (fix)	—	—	100 \pm 20	—	1.29 $^{+0.22}_{-0.11}$	27/35
December 07+09 ³	3	1.50 (fix)	—	1.60 $^{+0.38}_{-0.15}$	—	1.28 $^{+4.30}_{-0.85}$	1.26 $^{+0.29}_{-5.26}$	29/34
	3	8.14 $^{+1.49}_{-1.36}$	—	2.33 (fix)	—	1.76 (fix)	0.96 (fix)	48/37
	4	1.50 (fix)	2.92 $^{+6.07}_{-2.92}$	1.93 $^{+0.58}_{-0.42}$	—	1.16 $^{+0.30}_{-0.19}$	1.27 $^{+0.27}_{-0.15}$	25/34
	1	1.50 (fix)	—	1.57 \pm 0.05	—	—	—	60/47
December 20	2	1.50 (fix)	—	—	103 $^{+23}_{-19}$	—	1.23 $^{+0.23}_{-0.12}$	38/43
	3	2.27 $^{+3.85}_{-1.80}$	—	1.73 $^{+0.64}_{-0.23}$	—	2.01 $^{+1.88}_{-0.65}$	1.29 $^{+0.41}_{-0.71}$	54/43
	4	1.50 (fix)	6.93 $^{+7.91}_{-5.96}$	2.45 $^{+0.79}_{-0.73}$	—	1.08 $^{+1.10}_{-0.15}$	1.34 $^{+0.23}_{-0.61}$	41/42
	1	1.50 (fix)	—	2.07 $^{+0.11}_{-0.20}$	—	—	—	22/12
December 21	4	1.50 (fix)	2.86 $^{+6.80}_{-2.80}$	2.47 $^{+0.62}_{-0.42}$	—	1.68 (fix)	0.96 (fix)	18/11
	1	1.50 (fix)	—	1.96 $^{+0.16}_{-0.15}$	—	—	—	29/17
	1	4.44 $^{+3.25}_{-2.67}$	—	2.33 $^{+0.43}_{-0.37}$	—	—	—	26/16
	2	1.50 (fix)	—	—	110 \pm 14	—	0.92 $^{+0.37}_{-0.56}$	16/15
December 20+21 ³	4	1.50 (fix)	12.42 $^{+9.91}_{-6.72}$	3.38 $^{+1.00}_{-0.73}$	—	1.30 $^{+0.43}_{-0.26}$	0.98 $^{+0.73}_{-0.95}$	12/14
	1	1.50 (fix)	—	2.00 $^{+0.13}_{-0.12}$	—	—	—	52/30
	1	3.30 $^{+2.42}_{-2.10}$	—	2.22 $^{+0.31}_{-0.21}$	—	—	—	57/29
	2	1.50 (fix)	—	—	101 \pm 13	—	1.13 $^{+0.37}_{-0.39}$	33/27
	3	7.80 $^{+4.31}_{-3.60}$	—	3.05 $^{+0.70}_{-0.55}$	—	1.20 $^{+0.49}_{-0.20}$	1.28 $^{+0.44}_{-0.73}$	32/27
	4	1.50 (fix)	11.61 $^{+7.49}_{-5.73}$	3.41 $^{+0.78}_{-0.64}$	—	1.17 $^{+0.34}_{-0.17}$	1.32 $^{+0.45}_{-0.52}$	30/27

¹Model fit to the data: 1) Single power law with Galactic absorption; 2) Blackbody plus power law with Galactic absorption; 3) Broken power law with Galactic absorption; 4) Broken power law with Galactic absorption and intrinsic absorption at $z=0.121$

²This spectral slope also refers to the 0.3-10.0 keV slope in case only a single power law has been used.

³Simultaneous fits in *XSPEC*

TABLE 3

SPECTRAL PARAMETERS OF THE FITS TO THE ROSAT AND ASCA SPECTRA OF RX J0148.3-2758

Mission	observation	Model ¹	$N_{\text{H,Gal}}^2$	$N_{\text{H,intr}}^2$	$\alpha_{\text{X,soft}}^3$	kT^4	E_{break}^5	$\alpha_{\text{X,hard}}$	χ^2/ν
ASCA		1	1.50 (fix)	—	$1.48^{+0.09}_{-0.08}$	—	—	—	254/237
		2	1.50 (fix)	—	—	127^{+16}_{-20}	—	$1.10^{+0.13}_{-0.14}$	208/235
		3	1.50 (fix)	—	$2.03^{+0.23}_{-0.20}$	—	$1.36^{+0.16}_{-0.19}$	$1.11^{+0.16}_{-0.19}$	210/235
ROSAT	RASS	1	1.50 (fix)	—	$2.12^{+0.11}_{-0.11}$	—	—	—	30/23
		1	2.54 ± 0.82	—	2.62 ± 0.30	—	—	—	21/22
ROSAT	po	1	1.50 (fix)	—	1.88 ± 0.03	—	—	—	178/110
		1	2.35 ± 0.22	—	2.25 ± 0.08	—	—	—	111/110

¹Model fit to the data: 1) Single power law with Galactic absorption; 2) Blackbody plus power law with Galactic absorption; 3) Broken power law with Galactic absorption; 4) Broken power law with Galactic absorption and intrinsic absorption at $z=0.121$

²Column density N_{H} given in units of 10^{20} cm^{-2}

³This spectral slope also refers to the 0.3-10.0 keV slope in case only a single power law has been used.

⁴ kT in units of eV

⁵Broken Power law break energy E_{break} in units of keV

TABLE 4

UVOT PHOTOMETRY FROM THE CO-ADDED IMAGES OF RX J0148.3-2758

Filter	Segment 008		Segment 009		Segment 010		Segment 011	
	Mag	Flux ¹						
V	15.358 ± 0.062	26.90 ± 1.18	15.350 ± 0.018	27.10 ± 0.35	15.321 ± 0.020	27.84 ± 0.39	15.299 ± 0.017	28.41 ± 0.34
B	—	—	15.645 ± 0.015	33.45 ± 0.41	15.647 ± 0.017	33.37 ± 0.39	15.652 ± 0.088	33.24 ± 2.40
U	14.625 ± 0.042	47.19 ± 1.62	14.482 ± 0.011	53.80 ± 0.49	14.480 ± 0.013	53.91 ± 0.55	14.523 ± 0.030	51.81 ± 1.27
UVW1	14.531 ± 0.031	64.62 ± 1.52	14.485 ± 0.009	67.39 ± 0.49	14.471 ± 0.011	68.29 ± 0.56	14.425 ± 0.024	71.25 ± 1.32
UVM2	14.701 ± 0.031	74.77 ± 1.71	14.602 ± 0.010	81.85 ± 0.57	14.603 ± 0.011	81.78 ± 0.64	14.647 ± 0.024	78.57 ± 1.37
UVW2	14.598 ± 0.018	112.15 ± 1.46	14.537 ± 0.007	118.60 ± 0.59	14.530 ± 0.008	119.39 ± 0.66	14.533 ± 0.006	119.11 ± 0.56

¹The Fluxes are given in units of $10^{-19} \text{ W m}^{-2} \text{ \AA}^{-1}$

TABLE 5

UVOT PHOTOMETRY FROM THE CO-ADDED IMAGES OF THE FOUR COMPARISON STARS

Star	segment	V	B	U	UVW1	UVM2	UVW2
1	008	13.102 ± 0.036	—	13.695 ± 0.038	15.063 ± 0.041	16.842 ± 0.087	16.804 ± 0.050
	009	13.072 ± 0.011	13.638 ± 0.018	13.600 ± 0.010	15.058 ± 0.012	16.667 ± 0.024	16.729 ± 0.017
	010	13.074 ± 0.012	13.634 ± 0.020	13.599 ± 0.012	15.046 ± 0.013	16.670 ± 0.027	16.728 ± 0.020
	011	13.074 ± 0.010	13.676 ± 0.010	13.600 ± 0.028	15.026 ± 0.031	16.672 ± 0.061	16.707 ± 0.016
2	008	13.79 ± 0.037	—	14.29 ± 0.040	15.56 ± 0.056	16.96 ± 0.100	17.20 ± 0.063
	009	13.81 ± 0.011	14.38 ± 0.013	14.20 ± 0.011	15.60 ± 0.016	16.96 ± 0.029	17.20 ± 0.023
	010	14.02 ± 0.013	14.62 ± 0.014	14.42 ± 0.012	15.78 ± 0.019	17.17 ± 0.036	17.40 ± 0.028
	011	14.00 ± 0.011	—	—	—	—	17.36 ± 0.024
3	008	15.09 ± 0.057	—	15.57 ± 0.061	16.70 ± 0.114	18.90 ± 0.382	18.41 ± 0.157
	009	15.09 ± 0.016	15.66 ± 0.015	15.50 ± 0.015	16.87 ± 0.032	18.14 ± 0.060	18.50 ± 0.053
	010	15.05 ± 0.018	15.63 ± 0.017	15.55 ± 0.017	16.84 ± 0.035	18.20 ± 0.069	18.50 ± 0.061
	011	15.08 ± 0.016	15.74 ± 0.092	15.54 ± 0.042	16.80 ± 0.080	18.27 ± 0.160	18.41 ± 0.048
4	008	16.77 ± 0.162	—	16.89 ± 0.126	17.45 ± 0.196	18.34 ± 0.249	18.13 ± 0.120
	009	16.70 ± 0.038	17.02 ± 0.028	16.84 ± 0.023	17.52 ± 0.047	18.09 ± 0.056	18.38 ± 0.048
	010	16.69 ± 0.043	17.02 ± 0.031	16.85 ± 0.033	17.53 ± 0.053	18.12 ± 0.062	18.40 ± 0.053
	011	16.68 ± 0.036	17.16 ± 0.174	16.74 ± 0.073	17.45 ± 0.116	18.02 ± 0.131	18.33 ± 0.044

TABLE 6
MEASUREMENTS OF THE SPECTRAL ENERGY DISTRIBUTION SHOWN IN FIGURE 9.

Observatory	Filter	λ_c ¹	$\log \nu$ [Hz]	Magnitude ²	$\log \nu L_\nu$ ³	Comments
NVSS	1.40 GHz	—	9.146	<1mJy	4	
IRAS	100 μ m	100 μ m	12.477	746 \pm 190 mJy	7.41 \pm 1.89	
	60 μ m	60 μ m	12.699	237 \pm 50 mJy	3.98 \pm 0.83	
	25 μ m	25 μ m	13.079	107 \pm 25 mJy	4.27 \pm 1.00	
	12 μ m	12 μ m	13.398	113 \pm 30 mJy	9.55 \pm 2.54	
2MASS	Ks	2.159 μ m	14.143	12.250 \pm 0.026	3.85 \pm 0.05	
	H	1.662 μ m	14.302	13.399 \pm 0.032	2.99 \pm 0.10	
	J	1.235 μ m	14.385	14.214 \pm 0.025	2.67 \pm 0.07	
UVOT	V	5460 \AA	14.740	15.37 \pm 0.02	5.08 \pm 0.25	Segment 010
	B	4340 \AA	14.840	15.66 \pm 0.02	4.84 \pm 0.24	Segment 010
	U	3450 \AA	14.939	14.49 \pm 0.01	6.22 \pm 0.31	Segment 010
	UVW1	2600 \AA	15.062	14.49 \pm 0.01	5.88 \pm 0.30	Segment 010
	UVM2	2200 \AA	15.135	14.60 \pm 0.01	6.01 \pm 0.30	Segment 010
	UVW2	1930 \AA	15.191	14.54 \pm 0.01	7.70 \pm 0.38	Segment 010

¹Central wavelength of the filter

²For the NVSS and the IRAS data we give the flux densities in units of mJy. All others are given in units of mag.

³Observed Luminosities are given in units of 10^{37} W.

⁴The upper limit of the NVSS observation is $\nu L_{1.4GHz} < 4.7 \times 10^{31}$ W.